Numerical study of rocket upper stage deorbiting using passive electrodynamic tether drag

Alexandru IONEL*

*Corresponding author
INCAS – National Institute for Aerospace Research "Elie Carafoli"
B-dul Iuliu Maniu 220, Bucharest 061126, Romania
alexandru.ionel@incas.ro

DOI: 10.13111/2066-8201.2014.6.4.5

Abstract: *The purpose of this article is a numerical study of the possibility of deorbiting a rocket upper stage from low Earth orbit at EOM (end of mission) by means of passive electrodynamic tether drag. The article is structured as follows: the introduction presents the space debris problem in low Earth orbit and the possible methods of deorbiting spacecraft. The next part of the article describes summarily some space tether applications. The third part of the article presents the principle of operation behind passive electrodynamic tether drag. In the fourth part, this principle is detailed so as to represent the input for a numerical study for the deorbit time when using the passive electrodynamic drag concept as deorbiting application. Lastly, the results are presented and conclusions are drawn.*

Key Words: *upper stage, magnetic dipole, tether, deorbit, orbital debris, passive electrodynamic drag, reentry*

1. INTRODUCTION

Space debris has been growing rapidly since the start of the Space Age, which began in 1957 with the launch of the Soviet Union's first satellite, Sputnik 1. According to [1], in 2013 there were about 17000 object with sizes greater than 10 cm in LEO. These objects consist of spent rocket stages or satellites, but also collision fragments and various used spacecraft parts such as fuel containers, pipes, etc.

The debris poses a threat to on-going and future space missions (there are currently 655 satellites in LEO) and mitigations like the 25-year post-mission disposal [2] have been imposed so as not to further expand the debris objects number.

The historical practice of abandoning spacecraft and upper stages at EOM (end-of-mission) has allowed more than 2 million kg of debris to accumulate in LEO. The most effective means for preventing future collisions is the removal of all spacecraft and upper stages from the environment in a timely manner. Post mission disposal options are natural or directed reentry into the atmosphere within a specified time frame, a maneuver to one set of disposal regions in which the space structures will pose little threat to future space operations, and retrieval and return to Earth. In general, the most energy-efficient means for disposal of space structures in orbits below 1400 km is via maneuver to an orbit from which natural decay will occur within 25 years of EOM and 30 years from launch.

The re-entry orbit can also be reached by the use of certain re-entry oriented devices. These devises include passive devices such as decelerating sails (solar radiation pressure and drag-augmentation sails), tethers or balloons, devices for active control of the de-orbiting ballistic phase, such as aero brakes, ballast masses, flaps or parachutes and finally, additional propulsion sub-systems.

This article focuses on the use of a passive electro-dynamic drag tether as a means of de-orbiting an upper stage at EOM from a circular orbit in LEO, with an inclination up to 75 degrees.

2. TETHER APPLICATIONS IN SPACE MISSIONS

As pointed out in [3], the use of tether technology in space missions can be grouped in eight categories of applications, categories which specify the scientific field which utilizes tether technologies in space missions. These categories are the following: aerodynamics (i.e. station tethered express payload systems, multiprobe for atmospheric studies), concepts (i.e. gravity wave detections using tethers, Earth-Moon tether transport systems), controlled gravity (i.e. rotating controlled gravity laboratory, tethered space elevator), electrodynamics (i.e. electrodynamic power generation, electrodynamic thrust generation), planetary (i.e. Jupiter inner magnetosphere maneuvering vehicle, Mars tethered observer), science (i.e. science applications tethered platform, tethered satellite for cosmic dust collection), space station (i.e. microgravity laboratory, attitude stabilization and control), transportation (i.e. tether reboosting of decaying satellites, tether rendezvous system).

Electrodynamic applications of tethers include electrodynamic power generation, electrodynamic thrust generation and ULF/ELF/VLF communications antenna. The possible use of the electrodynamic power generation or electrodynamic brake/drag concept is the generation of DC electrical power to supply primary power to on-board loads. A description of the applied concept is the following: a spacecraft is connected to a subsatellite through an insulated conducting tether, with plasma contactors used at both tether ends, and the motion through the geomagnetic field induces a voltage across the tether, so that DC electrical power is generated at the expense of spacecraft/tether orbital energy. The space missions which proved the electrodynamic brake/drag concept were TSS-1 (1992), TSS-1R (1996) and the PMG (Plasma Motor Generator) flights (1993).

The electrodynamic power generation concept and practice showed that a tethered space system of mass 900 to 19000 kg, having an aluminum tether of length 10 to 20 km produces approximately 1kW to 1MW power.

The generation of electrodynamic thrust can be used to boost the orbit of a spacecraft. Concept description: current from a spacecraft’s on-board power supply is fed into the conducting, insulated tether (which connects the spacecraft and a possible subsatellite) against the electromagnetic force induced by the geomagnetic field, producing a propulsive force on the spacecraft/tether system. The TSS-1, TSS-1R and PMG missions have demonstrated this principle. The application of the generation of electrodynamic thrust concept implies that a tethered system of mass between 100 and 20000 kg, having am aluminum tether of length between 10 and 20 km produces thrust of up to 200 N, being powered with up to 1.6 MW.

3. PASSIVE ELECTRODYNAMIC TETHER DRAG - PRINCIPLE OF OPERATION

The electrodynamic drag concept is based on the exploitation of the Lorentz force due to the interaction between the electric current flowing in a conducting tether and the geomagnetic field. The motion of the conducting tether through the Earth’s magnetic field will generate a voltage along the tether. The electromagnetic interaction of a conducting tether deployed from an upper stage launcher vehicle at EOM (end of mission), moving at orbital speeds across Earth's magnetic field will induce current flow along the tether, provided there exists a means for the tether to make electrical contact with the ambient plasma, such as a hollow cathode plasma contactor, field emission device or a bare wire anode. The electron current is leaving the space plasma and entering the tether near the end so the current will flow upwards through the tether, towards the upper stage body.

The movement of the tether carrying a current I, while being embedded in a magnetic field B, will generate an electro-dynamic force F_E on each element of the tether. This force is always at right angles to both the magnetic field vector and the length vector of the tether, despite the variation of the angle α between the length vector of the tether and the local vertical (in the tether frame of reference), to which the orbital velocity vector of the upper stage launcher vehicle is perpendicular. The resultant electro-dynamic drag force is a component of the electro-dynamic force and is parallel to the velocity vector of the upper stage launcher vehicle but opposite in direction.

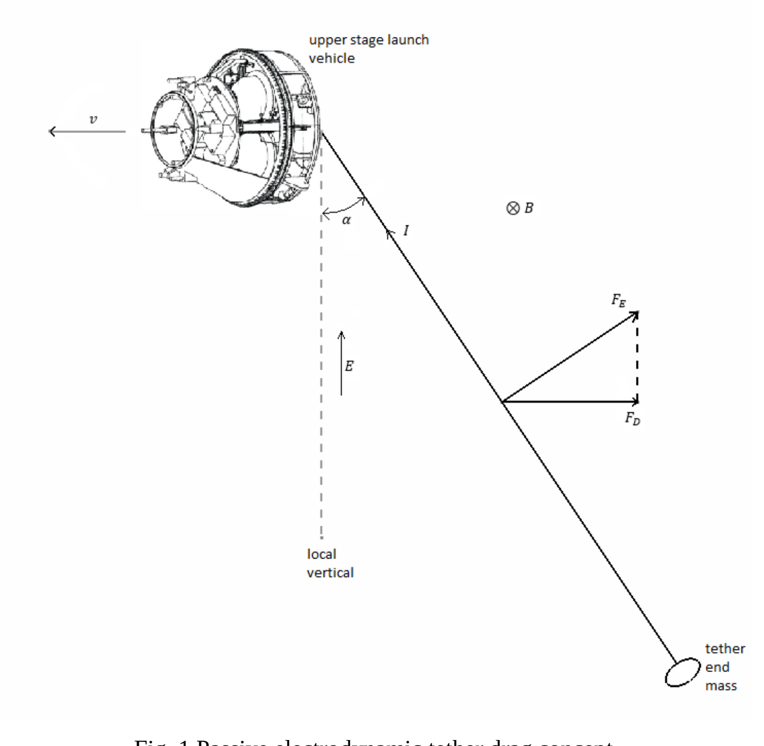

Fig. 1 Passive electrodynamic tether drag concept

4. ANALYSIS OF UPPER STAGE – TETHER SYSTEM IN ORBIT

In reference [2], it is found that a conducting tether which has the mass m_T, and is orbiting above the equator through a transverse magnetic field of strength B_T at a velocity with respect to the magnetic field v_M, will generate an electrical power P in the tether given by the following equation:

$$P = \frac{m_T (v_M B_T)^2}{rd} \tag{1}$$

$$\Delta t = \int_{a_1}^{a_2} \frac{\mu_\oplus m}{2a^2 P} da \tag{2}$$

In (1), r represents the resistivity and d is the density of the conducting material of which the tether is made of. The tether's resistance transforms this resulting power into heat, power which is then radiated away into space. This way, kinetic energy is extracted from the spacecraft. As specified in [4], a typical mass percentage of the tether, relative to the host spacecraft would be 1%. For an aluminium tether with mass $m_T = 15\,kg$, resistivity $r = 27.4\ n\Omega/m$ and density $d = 2700\ kg/m^3$, orbiting above the equator at a velocity of $v_M = 7000\ m/s$ relative to the Earth's transverse magnetic field $B_T = 20\,\mu T$, the power which will be dissipated will be $P = 2650\,W$. We can use this value, coupled with (2), from [5], to find out the time needed to lower a spacecraft's circular orbit from radius a_2 to radius a_1 (with $a_2 > a_1$. In (2), a represents the spacecraft circular orbit's semi-major axis, $\mu_\oplus$ is the Earth's gravitational parameter, m is the mass of the spacecraft and P is the power dissipated by the drag force, given in (1). If we choose $m = 1000\,kg$, $a_2 = 7378\,km$, $a_1 = 6628\,km$ (a spacecraft descending from an orbit of initial altitude relative to Earth's surface of 1000 km, to a final altitude of 250 km), we get $\Delta t = 14.08$ days.

The Earth's magnetic field can be approximated by a magnetic dipole with the magnetic axis of the dipole tilted off from the spin axis of the Earth by$\varphi = 11.5$, as illustrated in Fig2. Using this magnetic dipole model, the magnetic field can be divided at any point in two components: a tangential, or horizontal component, B_H, and a radial, or vertical component, B_V.

$$B_H = \frac{B_E R_E^3}{r^3} \sin \Lambda \tag{3}$$

$$B_V = \frac{B_E R_E^3}{r^3} \cos \Lambda \tag{4}$$

In (3) and (4) B_E represents the magnitude of Earth's magnetic field on the magnetic equator at the surface of the Earth and is equal to $31\,\mu T$ or $0.31\,gauss$, $R_E = 6378\,km$ is Earth's radius, r is the radial distance of a point from the centre of the Earth and Λ is the magnetic latitude starting from the Earth's magnetic equator. The 436 km offset of the magnetic dipole center from Earth's center will not be taken into account. The calculations will be made with respect to the magnetic dipole frame of reference so the orbit inclination will have the formula $\lambda = i \pm \varphi$, where λ is the inclination between the orbit and the $x_M O y_M$ plane of the magnetic dipole frame of reference, i is the angle between the orbit and Earth's frame of reference's $x_E O y_E$ plane and φ is the angle between Earth's plane of reference axes and the magnetic dipole frame of reference axes. The values of the inclination λ go from $\lambda = i + \varphi$ to $\lambda = i - \varphi$ once a day, as the upper stage orbits the Earth.

The circular orbit of the rocket upper stage can be parameterized in Cartesian and spherical coordinates, in terms of the angle θ around the orbit normal, assuming a fixed orbit inclination angle λ.

$$\boldsymbol{r} = \begin{bmatrix} x \\ y \\ z \end{bmatrix} = r \begin{bmatrix} \cos \lambda \\ \cos \lambda \sin \theta \\ \sin \lambda \sin \theta \end{bmatrix} \tag{5}$$

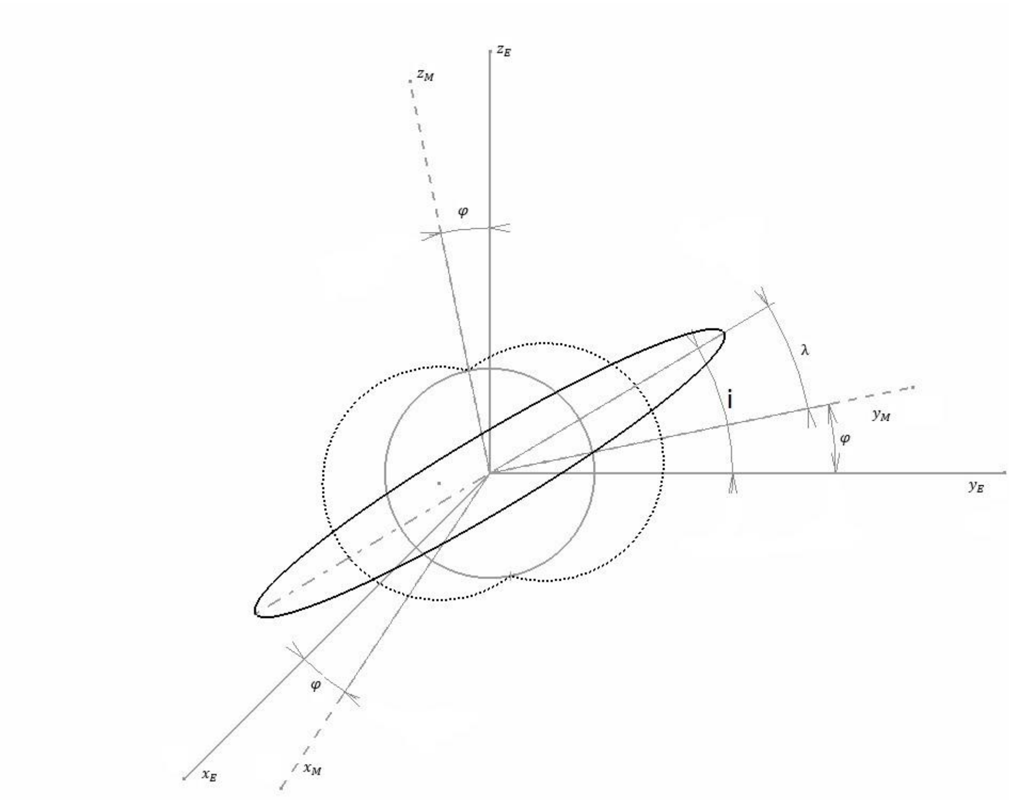

Fig. 2 Magnetic dipole model and orbit inclinations

The velocity of the rocket upper stage around the orbit, at a given point, by using (5) is found to be:

$$\boldsymbol{v} = v_0 \begin{bmatrix} -\sin\theta \\ \cos\lambda\sin\theta \\ \sin\lambda\cos\theta \end{bmatrix} \tag{6}$$

In (6), v_0 is the magnitude of the velocity around the orbit and is given by:

$$v_0 = \sqrt{\frac{GM_E}{r}} \tag{7}$$

In (5), $G = 6.67 \times 10^{-11}\ m^3/kg \cdot s^2$ and is Newton's gravitational constant and $M_E = 5.967 \times 10^{24}\ kg$ which is Earth's mass.

For better tracking of the calculations around the orbit, (5) can be used to describe in Cartesian and spherical coordinates the geomagnetic field.

$$\boldsymbol{B} = \frac{B_E R_E^3}{r^3} \begin{bmatrix} \frac{3xz}{r^2} \\ \frac{3yz}{r^2} \\ \frac{3z^2}{r^2} - 1 \end{bmatrix} = \frac{B_E R_E^3}{r^3} \begin{bmatrix} 3\sin\lambda\sin\theta\cos\theta \\ 3\sin\lambda\cos\lambda\sin^2\theta \\ 3\sin^2\lambda\sin^2\theta - 1 \end{bmatrix} \tag{8}$$

The motion of the tether across the geomagnetic field induces an electric field in the reference frame moving with the tether:

$$\boldsymbol{E} = -\boldsymbol{v} \times \boldsymbol{B} \tag{9}$$

Consequently, in the reference frame of the tether there will be a voltage along the tether:

$$\boldsymbol{V} = \boldsymbol{E} \cdot \boldsymbol{L} \tag{10}$$

In (7), the length vector of the tether has the following formula:

$$\boldsymbol{L} = L(\boldsymbol{r} \cos \alpha + \boldsymbol{v} \sin \alpha) \tag{11}$$

By coupling (4), (9) and (11) into (10) and keeping in mind that $\Lambda = \lambda$, now that we are doing the calculations in the magnetic dipole's frame of reference, we get the following formula for the voltage along the tether:

$$V = L \cos \alpha \, v_0 \frac{B_E R_E^3}{r^3} \cos \lambda \tag{12}$$

The hallow cathode plasma contactor, field emission device, or bare wire anode, mounted at the end of the tether provides contact with the ambient plasma to the tether and allows current to flow through it. The tether material has a total resistance R. This total resistance includes tether resistance, control circuit resistance, plasma contact resistance and parasitic resistances. The induced current flow through the tether will have the following formula:

$$\boldsymbol{I} = \frac{V}{R} \hat{\boldsymbol{L}} \tag{13}$$

The movement of the tether, through which an electrical current flows towards the upper stage launch vehicle body, through Earth's magnetic field, will generate an electrodynamic force (Lorentz force) on each element of the tether. When this force is integrated along the length of the tether, the net electrodynamic force F_E will be:

$$\begin{aligned} \boldsymbol{F_E} &= L(\boldsymbol{I} \times \boldsymbol{B}) = \frac{V}{R}(\boldsymbol{L} \times \boldsymbol{B}) = \frac{\boldsymbol{E} \cdot \boldsymbol{L}}{R}(\boldsymbol{L} \times \boldsymbol{B}) \\ &= \frac{(-\boldsymbol{v} \times \boldsymbol{B})\boldsymbol{L}}{R}(\boldsymbol{L} \times \boldsymbol{B}) = -\frac{1}{R} v_0 \frac{B_{\boldsymbol{E}} R_E^3}{r^{\boldsymbol{3}}} \cos \lambda \cdot L \cos \alpha \cdot L \frac{B_E R_E^3}{r^3} \\ &= -\frac{1}{R} v_0 L^2 \cos \alpha \frac{B_E^2 R_E^6}{r^6} (\cos \lambda)^2 \end{aligned} \tag{14}$$

Because of the tether's movement on orbit, an electrodynamic drag force F_D also appears, as component of the electrodynamic force F_E, being parallel but opposite in direction to the velocity vector. This electrodynamic drag force F_D has the following formula:

$$F_D = \boldsymbol{F_E} \cdot \hat{\boldsymbol{v}} = F_E \cos \alpha = -\frac{1}{R} v_0 \frac{B_E^2 R_E^6}{r^6} L^2 \cos^2 \alpha \cos^2 \lambda \tag{15}$$

Next, we can use this electrodynamic drag force F_D, (15), coupled with Lagrange's planetary equation for semi-major axis time-variation, (16), to find the total time needed for an electrodynamic tether to de-orbit an upper stage launcher vehicle, (17).

$$\frac{\partial a}{\partial t} = \frac{-2L^2 B_E^2 R_E^6 \cos^2 \alpha \cos^2 \lambda}{M_{US} R}\left(\frac{1}{a^5}\right) \tag{16}$$

In (16), a is the semi-major axis, t is the time and M_{US} is the mass of the upper stage.

$$\Delta t = \frac{M_{US} R}{12 L^2 B_E^2 R_E^2 \cos^2 \alpha \cos^2 \lambda} \tag{17}$$

5. NUMERICAL SIMULATION AND RESULTS ANALYSIS

Numerical simulations have been performed to investigate the de-orbit time of a rocket upper stage when using passive electrodynamic tether drag. The orbit was considered circular, the orbit inclinations used were considered to go from 0° to 75°, the mass of the rocket upper stage was presumed to range between 500 and 2000 kg, the tether length from 5 to 20 km and the altitudes from where the de-orbit procedure was started were considered to range from 500 to 2000 km (LEO upper limit).

All calculations were done from the altitude of reference to 250 km. According to [6], the angle between the tether and the local vertical in the tether frame of reference, maximizes the electrodynamic drag force when kept at $\alpha = 35.26°$.

This angle was used in the numerical application of this paper. The results obtained are comparable to the results obtained in [6] and [7].

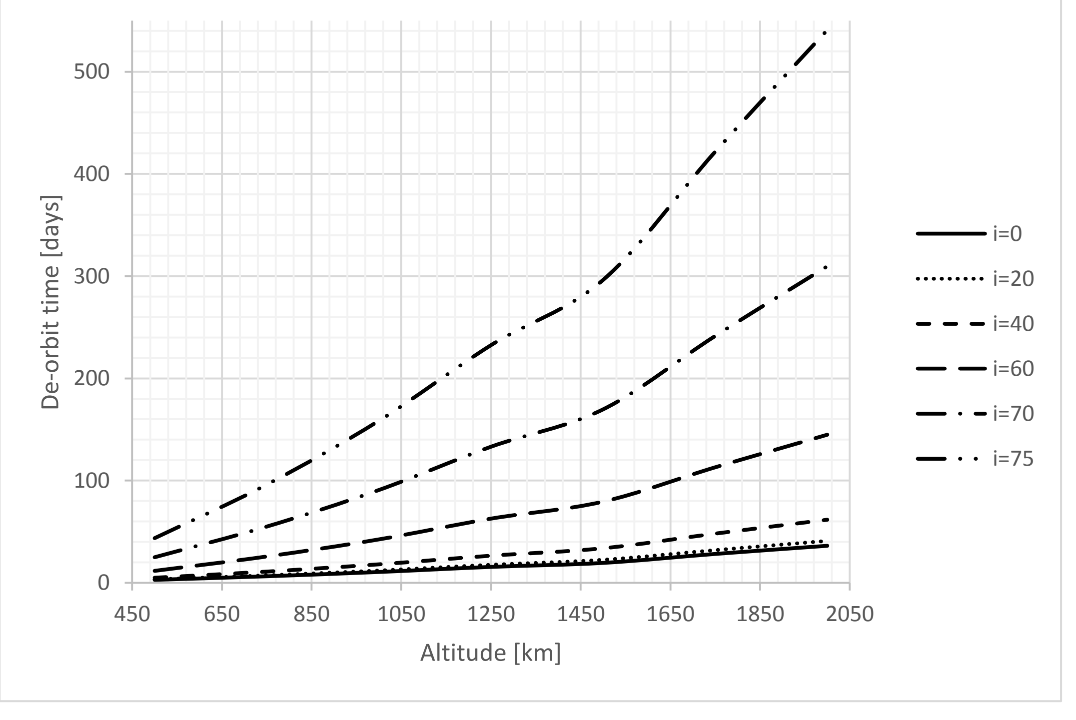

Fig. 3 De-orbit time depending on rocket upper stage altitude and orbit inclination wrt Earth's frame of reference. Tether length was considered to be $L = 10\ km$, tether diameter $D = 0.75\ mm$, $\alpha = 35.26°$, mass of rocket upper stage $M_{US} = 1000\ kg$

According to Fig. 3, the de-orbit time is greater for higher inclination orbits.

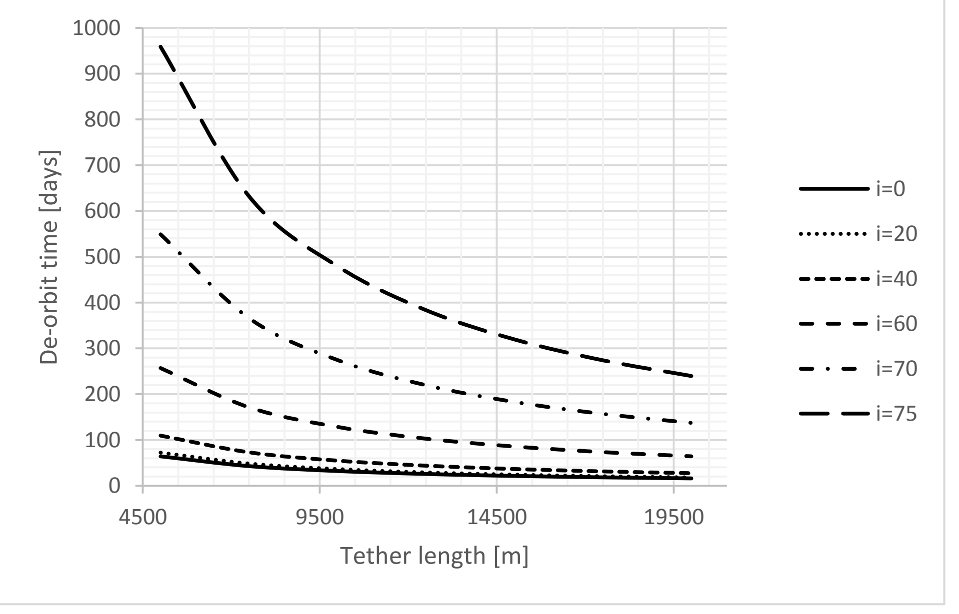

Fig. 4 De-orbit time depending on tether length and orbit inclination wrt Earth's frame of reference. The altitude considered was 1500 km, tether diameter $D = 0.75\ mm$, $\alpha = 35.26°$, mass of upper stage $M_{US} = 1500\ kg$

As it can be seen from Fig. 4 and Table 1, the de-orbit time is dependent upon tether length and orbit inclination. Consequently, longer tethers at less inclined orbits de-orbit faster. Fig. 5 describes how the de-orbit time is influenced by upper stage mass and tether length. De-orbit times will be larger for shorter tethers and heavier upper stages.

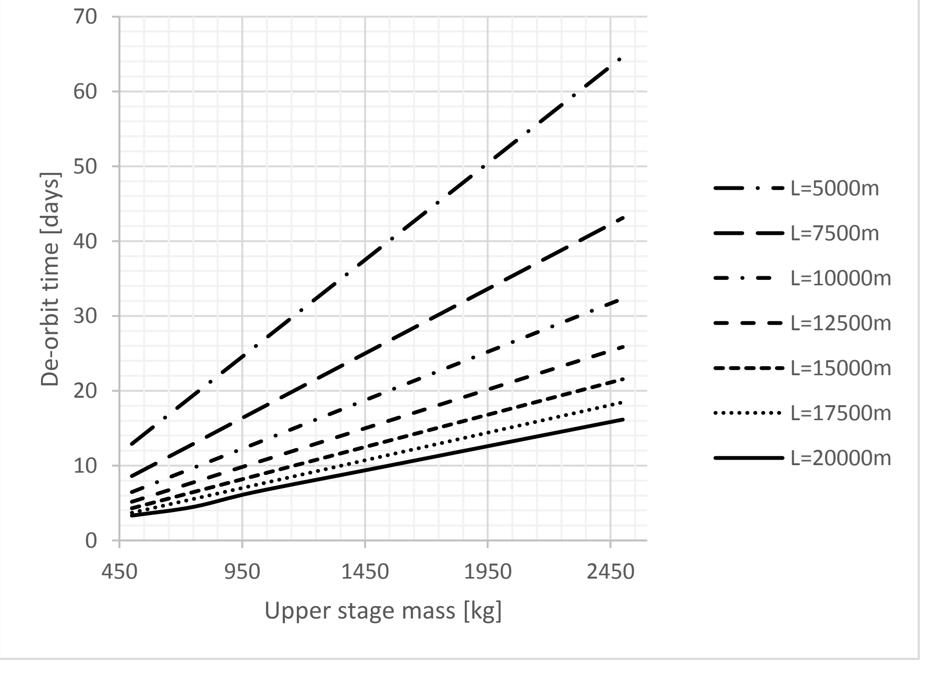

Fig. 5 De-orbit time depending on rocket upper stage mass and tether length. Orbit inclination was chosen to be $i = 25°$, tether diameter $D = 0.75\ mm$, $\alpha = 35.26°$

Table 1 shows F_D values and levels of voltage along the tether for different values of orbit inclination, tether length and tether diameter. The electrodynamic drag force decreases as inclination increases, as tether length decreases and as tether diameter decreases. This can also be seen from (15). The voltage through the tether decreases as orbit inclination increases and as the tether length decreases which is also highlighted by (12).

Table 1 – Electrodynamic drag force and voltage levels with different orbit inclination, tether length and tether diameter values. Altitude was chosen to be 2000 km, $\alpha = 35.26°$

$F_D\ [N]$	$V\ [V]$	$i\ [degrees]$	$L\ [km]$	$D\ [mm]$
0.123	385	0	5	1
0.289	577	0	7.5	1.25
0.456	698	25	10	1.5
0.472	680	45	12.5	1.75
0.739	817	45	15	2
0.37	577	60	15	2
0.181	348	75	17.5	2.5
0.297	398	75	20	3

Table 2 shows how power levels through the tether vary in accordance with tether mass, semi-major axis of the orbit, geomagnetic field value at tether position on orbit and orbit inclination.

Table 2 – Power levels and electrical resistance through a tether of mass m_T, length L, situated at the altitude r, on a circular orbit with inclination i

$m_{US}\ [kg]$	$m_T\ [kg]$	$L\ [km]$	$i\ [deg]$	$R\ [\Omega]$	$r\ [km]$	$B_T\ [\mu T]$	$P\ [W]$
500	5	5	0	369	750	22	1864
1000	10	7.5	25	416	1000	18.1	2406
1500	15	10	60	493	1500	8.2	694
2000	20	12.5	45	577	1750	10.5	1487
2500	25	15	75	665	800	5.6	594
3000	30	20	30	986	1250	15.6	5216

For de-orbit time comparison purposes, a numerical analysis on natural upper stage de-orbit time has also been performed (i.e. without the tether system). (18) describes the change in semi-major axis in one orbit revolution, due to atmospheric influence, and was coupled with (19), the number of revolutions, and the orbital period, (20) to find out the de-orbit time over many revolutions. Atmospheric data such as density, height scale, and temperature were obtained from [8] and [9]. The results are displayed in Table 3, for which have been chosen $i = 0$, the exospheric temperature $T = 1000\,K$, a tether with length $L = 15\,km$, $\alpha = 35.26°$, 1 mm thick aluminum tether and a circular orbit. Entry altitude was considered to be 250 km, as in the other calculations within this study. C_D, the atmospheric drag coefficient was considered to be 2, In (19), $BC = \frac{m_{US}}{C_D A}$ is the ballistic coefficient with A being the area of cross section perpendicular to the velocity of the upper stage.

The radius of this cross section was considered to be $r = 1.5\,m$. In (20), T is the mean orbital period and $\mu = G(m_{US} + M_E)$.

$$\Delta a = -2\pi \frac{\rho a^2 C_D A}{M_{US}} \tag{18}$$

$$n = 3 \cdot 10^{-4} BC \cdot e^{\frac{h}{H}} \quad (19)$$

$$T = 2\pi \frac{a^{3/2}}{\sqrt{\mu}} \quad (20)$$

Table 3 – Comparison between the reentry time of various mass upper stages at different altitudes with and without the tether de-orbitation system

M_{US} $[kg]$	H $[km]$	Reentry time without tether	Reentry time with tether
1000	500	58 years	1.1 days
1000	1000	9742 years	3.98 days
1000	2000	38880 years	13.58 days
1500	800	3458 years	4.05 days
1500	1500	14490 years	12.04 days
1500	2000	583000 years	20.37 days
2000	1000	19490 years	7.94 days
2000	1500	193200 years	16.05 days
2000	2000	777500 years	27.16 days

6. CONCLUSIONS

Although the passive electrodynamic tether drag proves, according to Fig. 3, Fig. 4, Fig. 5 and Table 3 highly efficient at increasing the orbital decay rate of an upper stage at EOM within LEO limits, its performance is highly dependent on orbit inclination, tether thickness, tether length, orbital stability and environment conditions. The higher the orbit inclination, the lower the strength of the geomagnetic field, thus the lower the electrodynamic drag force. Also, calculations with inclinations greater than $75°$ need to be treated differently as the spacecraft will advance in orbit in the retrograde direction relative to the magnetic field for a part of the day, the magnetic pole being rotated by the Earth's spin. Consequently, the voltage on the tether will have opposite direction for one portion of the day.

Tether thickness is important for current collection but can also provide safety from high speed orbital debris impacting the tether. The longer the tether, the smaller the de-orbit time, as suggested by Fig. 3, but this length can also be an environmental concern because a tethered spacecraft, as a whole, has a greater chance of colliding with other debris or spacecraft, thus creating more debris, malfunctioning satellites which are still in use or being a threat to on-going space missions.

REFERENCES

[1] * * * 50th Session of the Scientific and Technical Subcommittee United Nations Committee on the Peaceful Uses of Outer Space, *Stability of the future LEO environment*, *Report of an IADC study*, 11-22 February 2013.

[2] R. L. Forward, *Electrodynamic Drag Terminator Tether*, Appendix K, in Final Report on NAS8-40690.

[3] M. L. Cosmo and E.C. Lorenzini (eds), *Tethers in space handbook*, Third edition, Smithsonian Astrophysical Observatory, Cambridge, Massachusetts, USA, 1997.

[4] B. Barcelo and E. Sobel, *Space Tethers: Applications and Implementations*, PKA-SB07, February 2007.

[5] C. Pardini, T. Hanada, P. H. Krisko, *Benefits and risks of using electrodynamic tethers to de-orbit spacecraft*, IAC-06-B6.2.10.

[6] L. R. Forward, P. R. Hoyt and C. Uphoff, *Application of the Terminator Tether™ Electrodynamic Drag Technology to the Deorbit of Constellation Spacecraft*, AIAA Paper 98-3491, 34th Joint Propulsion Conference, July 1998.

[7] R. Hoyt and R. Forward, *The Terminator Tether™: Autonomous Deorbit of Leo Spacecraft for Space Debris Mitigation*, AIAA Paper 00-329, 38th Aerospace Sciences Meeting & Exhibit, Reno, Nevada, 10-13 January 2000.

[8] M. Nicolet, *Density of the Heterosphere Related to Temperature*, SAO Special Report #75, 1961.

[9] W. S. K. Champion, E. A. Cole and J. A. Kantor, *Standard and Reference Atmospheres*, Handbook of Geophysics and the Space Environment, Chapter 14, 2003.